# Fast disruptions by ballooning mode ridges and fingers in high temperature, low resistivity toroidal plasmas

Robert G. Kleva and Parvez N. Guzdar
*Institute for Plasma Research, University of Maryland, College Park, Maryland 20742-3511*

(Received 31 May 2000; accepted 16 October 2000)

The nonlinear evolution of ballooning modes in high temperature, low resistivity tokamaks is investigated. Convection cells driven by unstable ballooning modes rapidly convect the hot central plasma to the wall in ridges whose two-dimensional poloidal projection resembles fingers. As the resistivity $\eta$ is reduced in magnitude, the number of fingers increases, with the width of each individual finger becoming more narrow. Importantly, the rate at which energy is transported to the wall is unchanged as $\eta$ is reduced. Because of the increasingly fine scale fingers generated as $\eta$ is decreased, the time scale for diffusion across the fingers is independent of the magnitude of the resistivity. As a consequence, the magnetic field lines are decoupled from the plasma (not ''frozen-in'') even as $\eta$ approaches zero. The limit of resistive magnetohydrodynamics (MHD) as $\eta \rightarrow 0$ is not the same as ideal MHD with $\eta \equiv 0$. © *2001 American Institute of Physics.* [DOI: 10.1063/1.1331098]

## I. INTRODUCTION

The most serious impediment to the practical and economic utilization of tokamaks as fusion reactors is the limitation on the plasma thermal pressure imposed by disruptions. The ratio $\beta$ of the thermal pressure to the pressure of the confining magnetic field provides a measure of the efficiency of a magnetic confinement fusion reactor. Operation at high $\beta$ is very desirable because it yields a large fusion reaction rate relative to the cost of the confining magnetic field. However, experimental attempts to increase $\beta$ beyond a critical limit $\beta_c$ have been thwarted by an abrupt, catastrophic loss of confinement.[1] Just prior to this loss of thermal confinement during $\beta$ limit disruptions in tokamaks, small growing oscillations are observed on electron cyclotron emission detectors.[1,2] But these oscillations are only seen on detectors observing the large $R$ side of the torus, where $R$ is the major radius of the torus, and not on those observing the small $R$ side, indicating that the oscillations are ballooning in character. Our magnetohydrodynamic (MHD) simulations of tokamaks[3] have demonstrated that tokamaks at high $\beta$ are unstable to ballooning modes that grow on the pressure gradient on the large $R$ side of the torus. Nonlinearly, these ballooning modes develop into ridges of hot plasma and valleys of cold plasma that extend toroidally along the outside of the torus.[4] When projected onto a two-dimensional poloidal plane, these ridges and valleys have the appearance of fingers. The rate at which these fingers grow and transport energy is proportional to the magnitude of $\beta$.[4] At lower $\beta$ the fingers grow more slowly and are halted nonlinearly by a self-generated axisymmetric flow, and confinement is maintained.[4] But at higher $\beta$ the fingers grow too rapidly to be affected by the axisymmetric flow,[4] and the fingers of hot plasma rapidly convect across the magnetic field lines from the center of the discharge to the wall, thereby destroying confinement.[3] Simultaneously, fingers of cold edge plasma are injected across the magnetic field lines into the center of the discharge.

The gradients across the hot and cold plasma fingers in our MHD simulations are only limited by the magnitude of the plasma dissipation. The grid of computational points in our simulations must be chosen dense enough to resolve these gradients. Because there is only a finite amount of computer memory available, the dissipation in our earlier simulations[3] was necessarily large, much larger than that at the center of a hot tokamak, so that the gradients could be resolved with the available number of grid points. In order to account for the rapid loss of energy, on a timescale of about 100 $\mu$s, observed during the thermal quench in $\beta$ limit disruptions,[1] the rapid growth of hot plasma fingers from the center of the discharge to the wall seen in our earlier simulations[3,4] must persist as the dissipation is reduced in magnitude. Also, it has been claimed[5] that the convection of plasma across the magnetic field lines in our simulations is an artifact of the artificially large resistivity used, and that at smaller resistivity the plasma would be tied to the field lines. We address these issues in this paper by investigating the nonlinear evolution of ballooning modes as the dissipation is reduced.

In order to reduce the magnitude of the dissipation in our MHD simulations, a large increase in the number of grid points in the simulation is required, necessitating a large increase in computer memory. By using a parallel computer with multiple processors, we have been able to reduce the magnitude of the dissipation in our simulations by a factor of ten. From our MHD simulations of high $\beta$ tokamaks at reduced resistivity we draw the following major conclusions: (1) The rate at which the hot plasma fingers grow from the center of the discharge to the wall remains unchanged as the resistivity $\eta$ is reduced in magnitude. The growth rate is determined solely by the magnitude of $\beta$. (2) As the magnitude of the dissipation decreases, the number of plasma fingers generated increases while the width of each individual finger becomes more narrow. (3) The finger width decreases with $\eta$ as $\eta^{1/2}$. As a consequence, the time scale for diffusion across the fingers is independent of the magnitude of the resistivity. Thus, even though the resistivity is reduced in magnitude, the resistivity remains effective at decoupling the magnetic field lines from the plasma, and the narrower plasma fingers are still convected across the magnetic field lines.

The rest of this paper is organized as follows. The equations and numerical scheme that we use in our simulations are discussed in Sec. II. In Sec. III, we directly compare the nonlinear evolution of ballooning modes at both larger and smaller values of $\eta$. In Sec. IV, we demonstrate that the convection cells associated with nonlinear ballooning modes transport energy at a rate that is independent of the magnitude of $\eta$. The importance of resistive diffusion, even at small $\eta$, is shown in Sec. V. We summarize and discuss our results in Sec. VI.

## II. EQUATIONS AND NUMERICAL SCHEME

Our nonlinear simulations of high $\beta$ tokamaks are based on the resistive MHD equations for the magnetic field $\mathbf{B}$, the mass velocity $\mathbf{V}$, the temperature $T$, and the mass density $\rho_m$:

$$\partial \mathbf{B}/\partial t = \nabla\times(\mathbf{V}\times\mathbf{B}) + \eta\nabla^2\mathbf{B}, \tag{1}$$

$$\partial \mathbf{U}/\partial t + \nabla\cdot(\mathbf{V}\mathbf{U}) = \mathbf{J}\times\mathbf{B} - \nabla P + \mu\nabla^2\mathbf{U}, \tag{2}$$

$$\partial T/\partial t + \mathbf{V}\cdot\nabla T - \nabla_\parallel \kappa_\parallel \nabla_\parallel T = 0, \tag{3}$$

$$\partial \rho_m/\partial t + \nabla\cdot\mathbf{U} - D\nabla^2\rho_m = 0, \tag{4}$$

where the parallel gradient $\nabla_\parallel = \hat{\mathbf{b}}\cdot\nabla$ with $\hat{\mathbf{b}} = \mathbf{B}/|\mathbf{B}|$, the momentum density $\mathbf{U} = \rho_m\mathbf{V}$, the pressure $P = \rho_m T$, and the current $\mathbf{J} = \nabla\times\mathbf{B}$, for a plasma with resistivity $\eta$, viscosity $\mu$, parallel thermal conductivity $\kappa_\parallel$, and diffusion coefficient $D$. Equations (1)–(4) are solved in toroidal geometry $(R,\phi,z)$, where $R$ is the major radial coordinate of the torus, $\phi$ is the toroidal angle, and $z$ is the vertical distance along the axis of the torus, with a square conducting wall of half-width $a$ in the poloidal plane. The equations are given in normalized units[6] in which the time $t$ is normalized to the Alfvén time $\tau_A \equiv a/v_A$ with $v_A$ the Alfvén speed, and the resistivity $\eta = S^{-1}$ where the Lundquist number $S \equiv \tau_r/\tau_A$ is the ratio of the resistive diffusion time $\tau_r$ to the Alfvén time. In our simulations we consider a torus with aspect ratio $A \equiv R_0/a = 3$, where $R_0$ is the major radius of the torus. We generate a toroidal equilibrium with $\beta = 1.3\%$, where $\beta \equiv P_0/B_\phi^2(R = R_0)$ and $P_0$ is the pressure at the magnetic axis. In this equilibrium, the safety factor $q = 1.1$ at the magnetic axis and increases monotonically from the magnetic axis to the wall. The equilibrium mass density is uniform in space. The ion pressure is the dominant source of instabilities in high $\beta$ tokamaks since the bulk of the thermal energy resides in the ions. At the core of a large hot tokamak ($R_0 = 260$ cm, $a = 80$ cm, $B_\phi = 40$ kG, density $n = 5\times10^{13}$ cm$^{-3}$, central temperature $T = 10$ keV), the Alfvén time $\tau_A \approx 0.1$ $\mu$s and the ion–ion collision time $\tau_{ii} \approx 20$ ms $\approx 2\times10^5\tau_A$. On timescales shorter than $\tau_{ii}$, the ions are collisionless and stream freely down magnetic field lines. With a time-dependent parallel thermal coefficient $\kappa_\parallel = v_i^2 t$, where $v_i$ is the ion thermal velocity, the time scale $\tau_\parallel$ for the transport of energy a distance $s$ down a magnetic field line is given by the free-streaming result $\tau_\parallel = s/v_i$. The other transport coefficients ($\eta$, $\mu$, and $D$) are discussed in Sec. III.

We solve Eqs. (1)–(4) numerically on a three-dimensional set of grid points in $R$, $z$, and $\phi$. The number of grid points used in $(R,z,\phi)$ is $300\times300\times150$. Derivatives are evaluated using finite differences, and the equations are stepped forward in time using a leapfrog trapezoidal scheme. The equations are solved on a parallel computer with multiple processors.

## III. NONLINEAR BALLOONING MODE EVOLUTION

The high $\beta$ tokamak equilibrium is linearly unstable to ballooning modes with a broad unstable spectrum in toroidal mode number $n$.[3] These modes grow on the pressure gradient on the large $R$ side of the magnetic axis. Nonlinearly, the ballooning modes develop into a series of hot plasma ridges and cold plasma valleys, whose poloidal projection has the appearance of fingers. The nonlinear evolution of these fingers is shown in Fig. 1. This figure is a plot of the pressure in the poloidal plane at toroidal angle $\phi = 0$, at various times during the nonlinear evolution. The hottest, high pressure plasma is located in the red region. The pressure decreases progressively through the yellow, green, blue, and violet regions. The wall is located at the boundary of the violet region and the light blue region on the outside. Two different simulations are shown in Fig. 1. These simulations differ only in the magnitude of the transport coefficients. For the simulation on the left hand side of Fig. 1, the transport coefficients $\eta = \mu = D = 3\times10^{-4}$, while the transport coefficients for the simulation on the right hand side are only one-tenth as large: $\eta = \mu = D = 3\times10^{-5}$. The same initial perturbation is applied to the equilibrium in both cases.

When $\eta = 3\times10^{-4}$ ($S = 3.3\times10^3$), the perturbation grows and convects the hot central plasma out towards the wall at large $R$ in fingers. Most of the transport is dominated by two large fingers, one above the midplane $z = 0$ of the torus and the other below. (The up–down symmetry seen in Fig. 1 is a consequence of the up–down symmetry of the initial perturbation at $\phi = 0$; the poloidal projection of the pressure is not up–down symmetric at other toroidal angles.) Energy confinement is lost as the hot plasma fingers reach the wall.

When $\eta = \mu = D = 3\times10^{-5}$ ($S = 3.3\times10^4$), the perturbation grows and again convects the hot central plasma out towards the wall at large $R$ in fingers. But a larger number of fingers is generated nonlinearly at smaller $\eta$. For example, a hot plasma finger convects directly outward right along the midplane $z = 0$ when $\eta = 3\times10^{-5}$, while there is no hot plasma finger at the midplane $z = 0$ when $\eta = 3\times10^{-4}$. While the number of plasma fingers generated increases as $\eta$ becomes smaller, the width of each individual finger becomes more narrow. There are approximately three times as many fingers when $\eta = 3\times10^{-5}$ than when $\eta = 3\times10^{-4}$,

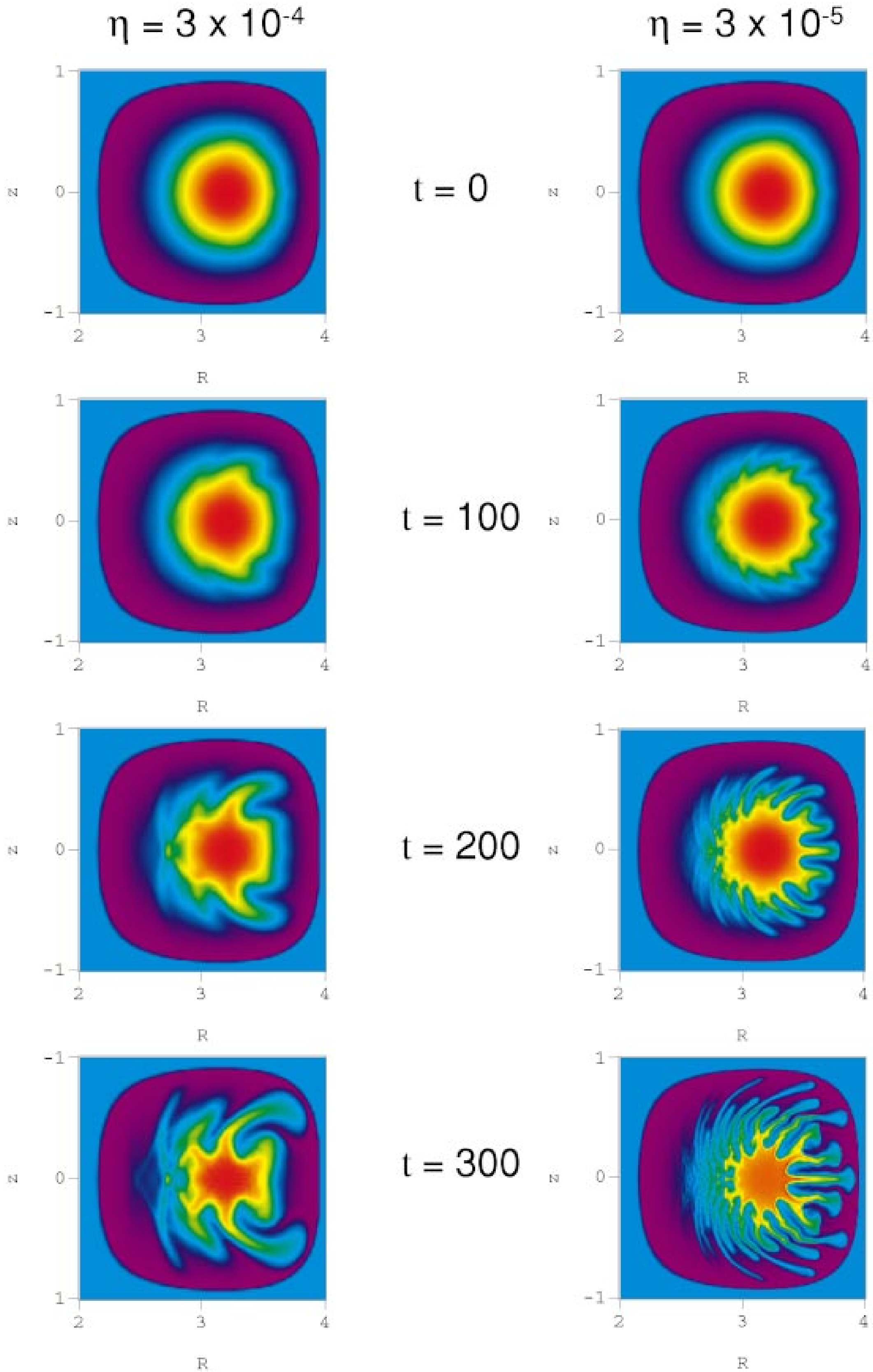


FIG. 1. (Color) Nonlinear ballooning modes. The series of plots shows the temporal evolution of the pressure $P$ in the poloidal plane $(R,z)$ at toroidal angle $\phi=0$. The hottest, high pressure plasma is located in the red region. The pressure decreases progressively through the yellow, green, blue, and violet regions. The wall is located at the boundary of the violet region and the light blue region on the outside. The transport coefficients $\eta=\mu=D=3\times10^{-4}$ for the simulation on the left, while $\eta=\mu=D=3\times10^{-5}$ for the simulation on the right.

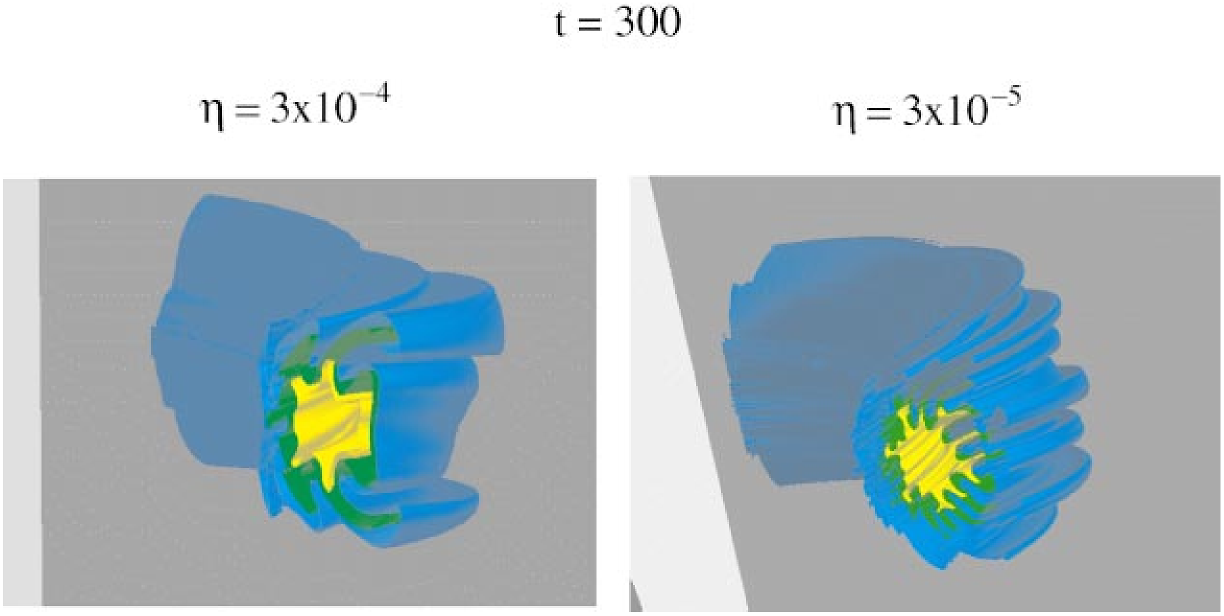


FIG. 2. (Color) Three-dimensional structure of the pressure. Three surfaces of constant pressure (yellow, green, and blue) are shown for one quarter of the torus ($\phi=0$ to $\phi=\pi/2$) at $t=300$, with the yellow surface the hottest of the three surfaces. The transport coefficients $\eta=\mu=D=3\times10^{-4}$ for the simulation on the left, while $\eta=\mu=D=3\times10^{-5}$ for the simulation on the right.

and the width of each individual finger is only about one third as large. The number $N$ of fingers evidently scales with $\eta$ as $N\sim\eta^{-1/2}$, while the width $w$ of each finger scales as $w\sim\eta^{1/2}$. Thus, there is more fine scale structure in the pressure as the dissipation decreases. But energy confinement is still lost at lower $\eta$ as the more numerous hot plasma fingers still reach the wall.

The full three-dimensional structure of the pressure in the two simulations is displayed in Fig. 2. This figure shows three surfaces of constant pressure (yellow, green, and blue) for one quarter of the torus ($\phi=0$ to $\phi=\pi/2$) at $t=300$, with the yellow surface the hottest of the three surfaces. A surface of constant pressure consists of a series of ridges and valleys that extend predominantly along the outside of the torus. The hot and cold fingers seen in Fig. 1 are two-dimensional projections onto the poloidal plane $\phi=0$ of these three-dimensional ridges and valleys.

## IV. THERMAL QUENCH TIME

A direct comparison of the temporal evolution of the pressure for the two different simulations shown in Fig. 1 demonstrates that the time scale over which energy confinement is lost is virtually the same in the two cases, even though $\eta$ differs by a factor of ten between the two simulations. In both cases the fingers of hot central plasma first reach the wall in approximately 300 Alfvén times, or about 30 $\mu$s for the tokamak parameters given in Sec. II. Since the hot central plasma is being convected out towards the wall at large $R$, as a quantitative measure of the rate at which confinement is destroyed we consider the maximum of the major radial component of the fluid velocity, $V_{R,\max}$. Figure 3 is a plot of $V_{R,\max}$, normalized to the Alfvén speed $v_A$, as a function of the time $t$ during the nonlinear evolution. The solid line in Fig. 3 shows the temporal dependence of $V_{R,\max}$ at smaller $\eta=3\times10^{-5}$, while the temporal dependence at larger $\eta=3\times10^{-4}$ is given by the dashed line. As the convection cells deepen and grow nonlinearly, the flow velocity towards the wall at large $R$ increases monotonically with time until the hot plasma fingers reach the wall. As a function of time, the maximum radial velocity $V_{R,\max}$ is nearly identical in the two cases. Although the resistivity $\eta$ is reduced by a factor of ten, the rate at which energy is transported to the wall is virtually unchanged.

## V. MAGNETIC FIELD

While the convection cells generated by the nonlinear ballooning modes distort the plasma thermal energy into fingers, at the same time the magnetic field is virtually unchanged from its equilibrium configuration. Vector plots of

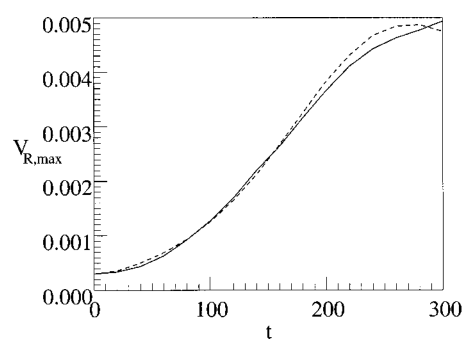


FIG. 3. Flow velocity to the wall. The temporal dependence of the maximum of the major radial component of the fluid velocity, $V_{R,\max}$, normalized to the Alfvén speed, $v_A$, is plotted. The solid line is the result for $V_{R,\max}(t)$ when $\eta=3\times10^{-5}$ while the dashed line is the result for $\eta=3\times10^{-4}$.

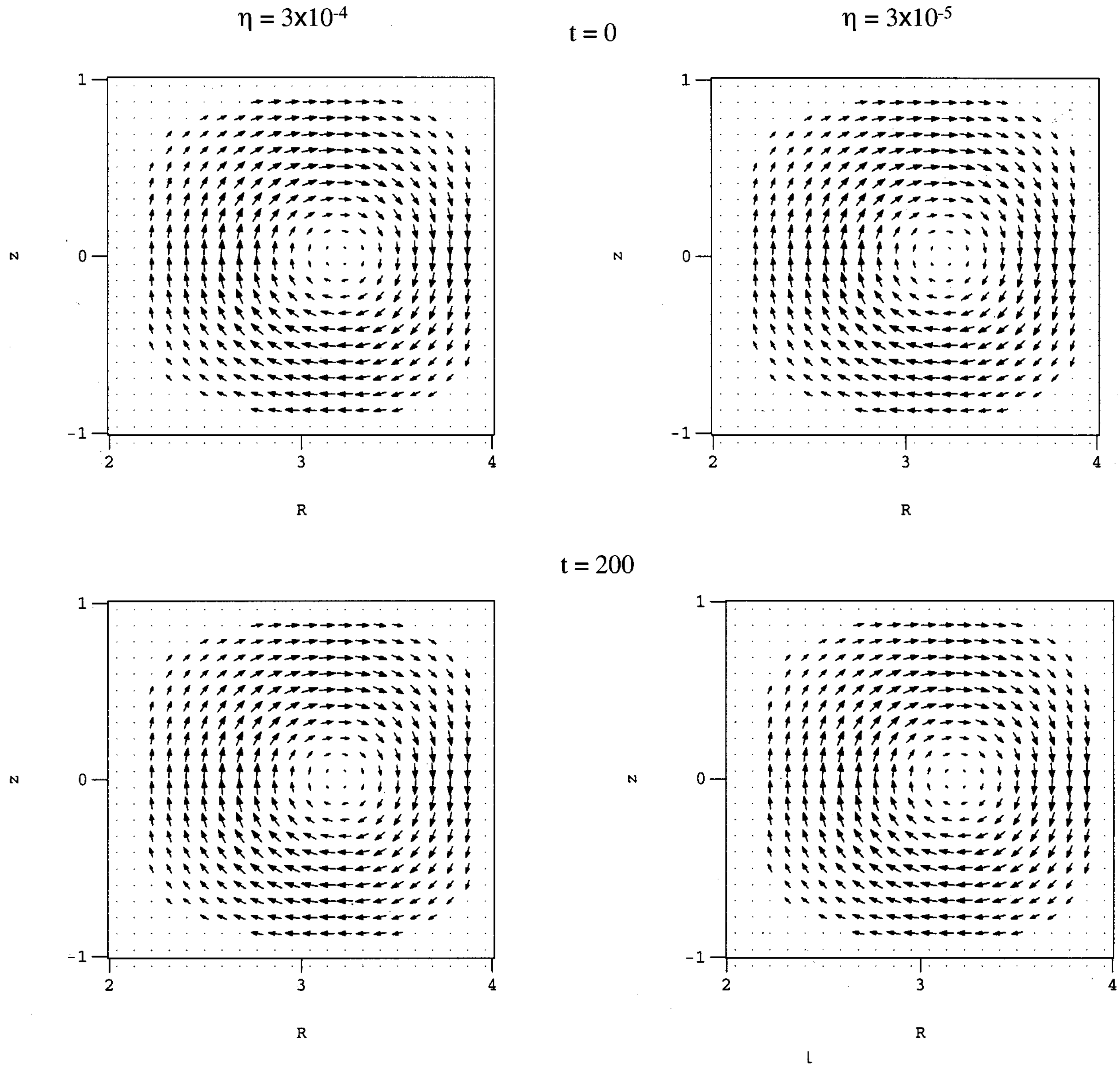


FIG. 4. Magnetic field. The temporal evolution of the poloidal magnetic field is shown in a series of vector plots in the poloidal plane $(R,z)$ at $\phi=0$ for $\eta=3\times10^{-4}$ (left hand side) and $\eta=3\times10^{-5}$ (right hand side).

the poloidal magnetic field at toroidal angle $\phi=0$ are shown in Fig. 4. The magnetic field plots on the left hand side of Fig. 4 are from the simulation with $\eta=3\times10^{-4}$, while the magnetic field plots from the $\eta=3\times10^{-5}$ simulation are shown on the right. In both cases, there is no discernable difference between the magnetic field at $t=200$ and the equilibrium magnetic field at $t=0$. While the plasma thermal energy has been distorted into fingers of hot and cold plasma (Fig. 1), no such fingers are seen in the magnetic field. In the ideal MHD approximation ($\eta\equiv0$), the magnetic field lines would be ''frozen-in'' to the flow and the convection cells would generate fingers in the magnetic field, like the fingers in the pressure. But in our resistive MHD simulations, the magnetic field lines have not been carried along with the plasma, but instead the plasma thermal energy has been convected across the magnetic field lines even as the resistivity $\eta$ is reduced.

What little effect the convection cells actually do have on the magnetic field can only be seen by subtracting the equilibrium magnetic field from the total magnetic field. Let us define the difference $\delta B_{\mathrm{pol}}\equiv B_{\mathrm{pol}}-B_{\mathrm{pol,eq}}$ between the poloidal magnetic field $B_{\mathrm{pol}}=(B_R^2+B_z^2)^{1/2}$ and the equilibrium poloidal magnetic field $B_{\mathrm{pol,eq}}$. A plot of the magnitude of $\delta B_{\mathrm{pol}}$ in the poloidal plane at $\phi=0$ is shown in Fig. 5. The fluctuation $\delta B_{\mathrm{pol}}$ from equilibrium is largest in the lighter areas and approaches zero in the dark areas. For both larger and smaller $\eta$, the fluctuation $\delta B_{\mathrm{pol}}$ from equilibrium is nonzero only in narrow regions around the location of the fingers in the plasma pressure. Over these narrow regions resistive diffusion is important even though the resistivity $\eta$ is small. As $\eta$ decreases, the regions where $\delta B_{\mathrm{pol}}$ is nonzero become even more narrow, so that the gradients in $\delta B_{\mathrm{pol}}$ become larger. For this reason, resistive diffusion remains important

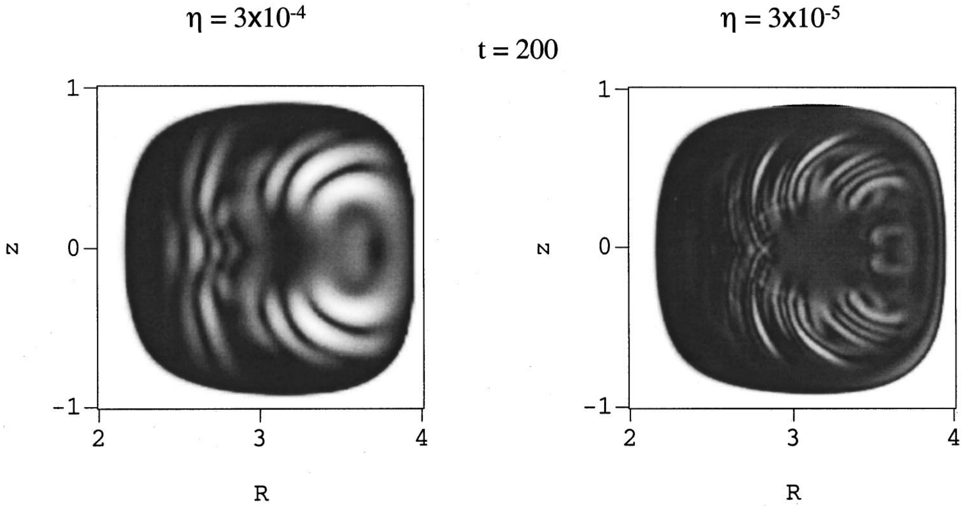


FIG. 5. Poloidal magnetic field fluctuation. The fluctuation $\delta B_{pol} \equiv B_{pol} - B_{pol,eq}$ of the poloidal magnetic field $B_{pol} = (B_R^2 + B_z^2)^{1/2}$ from the equilibrium field $B_{pol,eq}$ is plotted in the poloidal plane ($\phi = 0$) at $t = 200$ for $\eta = 3 \times 10^{-4}$ (left hand side) and $\eta = 3 \times 10^{-5}$ (right hand side). The fluctuation $\delta B_{pol}$ is largest in the lighter regions and near zero in the darker regions.

even as $\eta$ becomes smaller and, as a result, the magnetic field lines are not tied to the plasma and there are no fingers in the total magnetic field. As a measure of the magnitude of $\delta B_{pol}$ relative to the equilibrium poloidal magnetic field, we define the normalized poloidal magnetic field fluctuation $\delta\overline{B}_{pol}$ as the square root of the ratio of the volume average of $\delta B_{pol}^2$ to the volume average of $B_{pol,eq}^2$: $\delta\overline{B}_{pol} \equiv (\int \delta B_{pol}^2 dV / \int B_{pol,eq}^2 dV)^{1/2}$. The solid line in Fig. 6 is the temporal dependence of $\delta\overline{B}_{pol}$ when $\eta = 3 \times 10^{-5}$, while the dashed line is the result when $\eta = 3 \times 10^{-4}$. Although $\eta$ differs by a factor of ten between the two cases, the results are nearly the same and the magnetic field fluctuation is only about 1% of the equilibrium field.

## VI. DISCUSSION

There are indeed important qualitative changes in the nonlinear evolution of ballooning modes in tokamaks as the resistivity of the plasma is reduced in magnitude. The convection cells generated by the ballooning modes transport the hot central plasma to the wall at large $R$ in ridges whose two-dimensional poloidal projection resembles fingers. As the resistivity decreases, there is an increase in the number of convection cells and an increase in the number of hot plasma fingers being transported to the wall. Concomitantly, the width of each individual finger becomes more narrow as $\eta$ decreases.

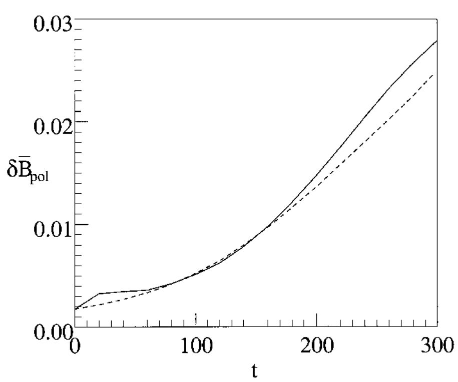


FIG. 6. Magnitude of the magnetic field fluctuation. The temporal dependence of the normalized poloidal magnetic field fluctuation $\delta\overline{B}_{pol}$ is plotted for $\eta = 3 \times 10^{-5}$ (solid line) and $\eta = 3 \times 10^{-4}$ (dashed line).

But these changes in the nonlinear structure of ballooning modes serve only to keep the important transport physics invariant as $\eta$ decreases. At reduced $\eta$, the fingers become more narrow and the gradients in the fingers steepen nonlinearly until resistive diffusion becomes large enough to balance this nonlinear steepening. Since the scale lengths in the magnetic field fluctuation are self-consistently determined by this balance between resistive diffusion and nonlinear steepening, resistive diffusion remains important even as the magnitude of $\eta$ is reduced. The time scale $\tau_d$ for diffusion across a finger of width $w$ is given by $\tau_d = w^2/\eta$. But as $\eta$ decreases the width $w$ of the fingers decreases as $w \sim \eta^{1/2}$. Thus, the time scale $\tau_d$ for diffusion across the fingers is independent of $\eta$. For nonlinear ballooning modes, the limit of resistive MHD as $\eta \rightarrow 0$ is not the same as ideal MHD with $\eta \equiv 0$ because resistive diffusion remains effective over the increasingly fine scale structure generated as $\eta \rightarrow 0$. As a consequence, the magnetic field lines are decoupled from the plasma (not ''frozen-in'') even as $\eta \rightarrow 0$, and the plasma fingers are convected across the magnetic field.

And, importantly, the rate at which energy is transported to the wall by the fingers is unchanged as $\eta$ is reduced in magnitude. This result is in marked contrast to disruption models based on magnetic stochasticity and/or magnetic reconnection. In resistive MHD, the rate of reconnection of magnetic field lines scales with the resistivity as $\eta^{1/2}$ and there is a large reduction in the reconnection rate as $\eta$ is reduced in magnitude.[7–9] But our nonlinear simulations demonstrate that confinement is destroyed by ballooning modes at a rate that is both independent of the magnitude of $\eta$, and is as rapid as the sudden loss of thermal confinement observed during $\beta$ limit disruptions.

Although our results strictly apply only to ballooning modes in a tokamak, these results may also be relevant to other MHD instabilities involving convection cells, like the Rayleigh–Taylor instability. Cowley and Artun[10] have investigated the nonlinear evolution of the Rayleigh–Taylor instability in an infinite slab geometry, using the ideal ($\eta \equiv 0$) MHD equations. In their calculations, the density is supported by straight magnetic field lines that are line-tied to a pair of parallel walls. From the momentum equation, they obtain an equation for the plasma displacement for a single Fourier mode. This equation is valid only when the wavelength of the mode is near zero, and only when the plasma is near marginal ideal stability. Their equation for the displacement is two-dimensional, and contains averages over the third dimension. Linearly, the plasma displacement of the Fourier mode exhibits a sinusoidal behavior in space. Nonlinearly, the peaks in the sinusoid steepen and resemble fingers. These fingers become infinitesimally narrow in a finite time. In contrast to these $\eta \equiv 0$ Rayleigh–Taylor results, we do not see a similar finite time singularity in our resistive ballooning mode calculations. In our calculations, the flow velocity increases with time but remains finite. Furthermore, the time dependence of the maximum flow velocity remains unchanged even as $\eta$ becomes small, so the system does not approach a finite time singularity as $\eta \rightarrow 0$. Again, the limit of resistive MHD as $\eta \rightarrow 0$ is not the same as ideal MHD with $\eta \equiv 0$.

## ACKNOWLEDGMENTS

We are grateful to Bill Dorland for providing his expertise on parallel computation. This research was supported by the U.S. Department of Energy.

[1] E. D. Fredrickson, K. McGuire, Z. Chang, A. Janos, M. Bell, R. V. Budny, C. E. Bush, J. Manickam, H. Mynick, R. Nazikian, and G. Taylor, Phys. Plasmas **2**, 4216 (1995).
[2] E. D. Fredrickson, K. M. McGuire, Z. Y. Chang, A. Janos, J. Manickam, G. Taylor, S. Mirnov, I. Semenov, D. Kislov, and D. Martynov, Phys. Plasmas **3**, 2620 (1996).
[3] R. G. Kleva and P. N. Guzdar, Phys. Rev. Lett. **80**, 3081 (1998).
[4] R. G. Kleva and P. N. Guzdar, Phys. Plasmas **7**, 1163 (2000).
[5] W. Park and E. D. Fredrickson, Phys. Rev. Lett. **82**, 5413 (1999).
[6] R. G. Kleva and P. N. Guzdar, Phys. Plasmas **6**, 116 (1999).
[7] P. A. Sweet, *Electromagnetic Phenomena in Cosmical Physics*, edited by B. Lehnert (Cambridge University Press, New York, 1958), p. 123.
[8] E. N. Parker, J. Geophys. Res. **62**, 509 (1957).
[9] D. Biskamp, Phys. Fluids **29**, 1520 (1986).
[10] S. C. Cowley and M. Artun, Phys. Rep. **283**, 185 (1997).